

Is the world running out of fresh water?

Tamma Carleton, Levi Crews, and Ishan Nath

ONLINE APPENDIX

A. Gravity Recovery and Climate Experiment

The Gravity Recovery and Climate Experiment (GRACE) satellite mission was launched in 2002 by the U.S. National Aeronautics and Space Administration (NASA) and the German Deutsche Forschungsanstalt für Luft und Raumfahrt (DLR). A “follow-on” mission to extend the satellite record was launched in 2018 and is ongoing. GRACE missions are composed of two identical space-craft, flying 220 km apart in the same orbital plane about 500 km above the Earth. The missions are designed to measure changes in Earth’s gravitational pull. As the pair passes over regions on Earth’s surface with greater mass, they will face stronger gravitational pull, affecting the distance between the lead and trailing satellites. Instruments on board generate precise measurements of the changing distance between the two satellites while in orbit, accurate up to one micrometer (μm) per second (Tapley et al., 2004).

Because water moves in large quantities through the hydrologic cycle at a rate far faster than other processes that move mass across the Earth’s surface, mass variations uncovered by GRACE are mostly attributable to changes in water content as it cycles between ocean, atmosphere, continents, glaciers, and polar ice caps (Tapley et al., 2004). This monthly output has been used to study ocean currents (Wahr, Jayne and Bryan, 2002), measure ground water storage on land (Rodell, Velicogna and Famiglietti, 2009), and document exchanges between ice sheets or glaciers and the oceans (Jacob et al., 2012), among many other applications. GRACE “solutions” of these monthly data – a solution converts distances between satellites into estimates of changing mass – are available in gridded form across the globe. We use the Goddard Space Flight Center (GSFC) mass concentration solution RL06v2.0, which converts time-variable gravity into centimeters of equivalent water height for 41,168 equal-area blocks, called mascons, which measure $1^\circ \times 1^\circ$ ($\sim 111.11\text{km} \times 111.11\text{km}$) at the equator (Loomis, Luthcke and Sabaka, 2019).

Following extensive scientific literature (e.g., Rodell, Velicogna and Famiglietti (2009); Richey et al. (2015); Rodell et al. (2018)), we assume that changes in mass recovered by GRACE can be treated as changes in total water storage (ΔTWS), which is composed of the following elements:

$$(A1) \quad \Delta\text{TWS} = \Delta\text{groundwater} + \Delta\text{surface water} + \Delta\text{soil moisture} + \Delta\text{snow water equivalent}$$

Throughout our analysis, we abstract from any decomposition of ΔTWS and directly use this aggregate measure of water storage.

GRACE has the important advantage of providing global-scale estimates of changes in total water availability; no other data product comes close to presenting such a comprehensive picture of changing water resources. However, like all remotely sensed data, there are many important limitations of the data. First, all changes in Earth’s gravitational field are recovered in GRACE, not only those due to changing water resources. For example, large landslides, mass human migrations, and large-scale mining activities, among other factors, can plausibly drive variation in gravitational pull. In our analyses, all of these changes are interpreted as changes in water resources. While this may appear limiting, prior research has documented that water dominates the overall variation in GRACE (Tapley et al., 2004), and that land surface and/or hydrologic models that are used to isolate specific components of GRACE (e.g., ground water) are highly sensitive to difficult-to-calibrate model parameters (Long et al., 2013). We therefore follow a large literature in interpreting gravitational anomalies from GRACE as changes in water resources and analyzing only aggregate TWS measures.

Second, the relatively low spatial resolution of GRACE ($1^\circ \times 1^\circ$) makes it valuable for global-scale analysis, but of limited use for many local water resource management questions. Other remotely sensed datasets, such as OpenET for measuring evapotranspiration (Melton et al., 2022) or InSAR

for measuring recharge (Neely et al., 2021), are available in some regions of the world and are undoubtedly more appropriate for certain applications.

Finally, GRACE gives a measure of changes in water storage, but not estimates of available water stocks. Changes in gravitational pull are estimated from GRACE by taking a residual relative to a modeled estimate of the geoid – the hypothetical shape of the Earth. The data are represented as *anomalies* in the average gravitational field, which prohibits any interpretation of output in levels. Moreover, because this method relies heavily on the modeled geoid, there is undoubtedly measurement error that may influence downstream empirical estimation (Proctor, Carleton and Sum, 2023).

B. Virtual Water Trade

We follow a standard approach to computing virtual water trade (d'Odorico et al., 2019). The virtual water trade for a single product k from a given country i to another country j , VWT_{ij}^k (m^3), is the product of the virtual water content of product k produced in country i , VWC_i^k (m^3/tonne), and the trade flow of crop k from i to j , Q_{ij}^k (tonnes). A country's net virtual water imports are then simply $nVWI_i = \sum_k \sum_j (VWT_{ji}^k - VWT_{ij}^k)$.

Data on trade flows for the year 2009 come from UN Comtrade. Products are defined at the HS6 level. We restrict our attention to crops and crop-derived food commodities. Country-specific estimates of virtual water content for each crop and crop-derived food commodity come from Mekonnen and Hoekstra (2011). These are calculated as the average ratio between total crop evapotranspiration in the growing season and annual crop yield over the years 1996–2005. We consider only the green and blue water content for each crop and commodity².

In total, our sample includes 228 distinct HS6 codes with non-zero virtual water flows in 2009. The top fifteen crops by virtual water flows—mostly cereals, oilseeds, and cotton lint—account for almost exactly 80% of the total volume.

²Green water is precipitation water directly contributing to the soil water balance in the crops' root zone in the absence of irrigation. Blue water is irrigation water withdrawn from surface water bodies and aquifers. Mekonnen and Hoekstra (2011) also provide estimates inclusive of grey water, which is the water volume required to dilute pollutants to a concentration that meets a given country's water quality standards. Including grey water does not qualitatively change our results.

C. Figures

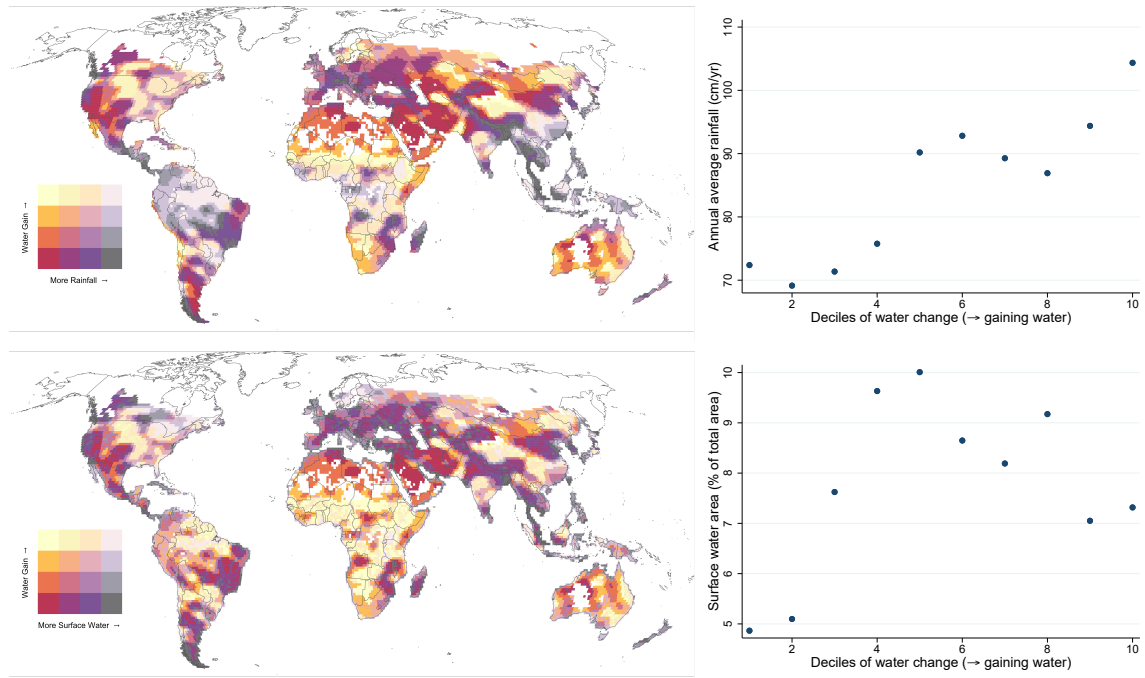


FIGURE A1. WATER LOSS AND BASELINE WATER AVAILABILITY

Note: Top panel: Map shows trends in total water storage (centimeters of equivalent water height per year) against average annual rainfall (centimeters per year). Plot shows average annual rainfall for each decile of trends in total water storage across global arable lands. Bottom panel: Map shows trends in total water storage against presence of surface water (percent of grid cell covered with surface water), derived from satellite-based estimates from [\(Pekel et al. 2016\)](#). Plot shows average surface water area for each decile of trends in total water storage across global arable lands.

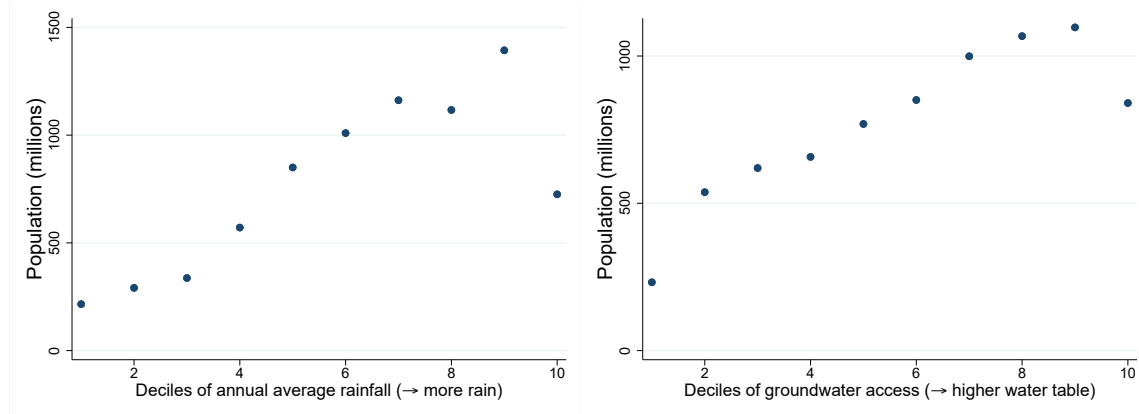


FIGURE A2. POPULATION EXPOSURE TO RAINFALL AND GROUNDWATER TABLE DEPTH

Note: Left panel plots the total population on arable land in each decile of the world's distribution of annual average rainfall. Right panel plots the total population on arable land in each decile of the world's groundwater table depth.

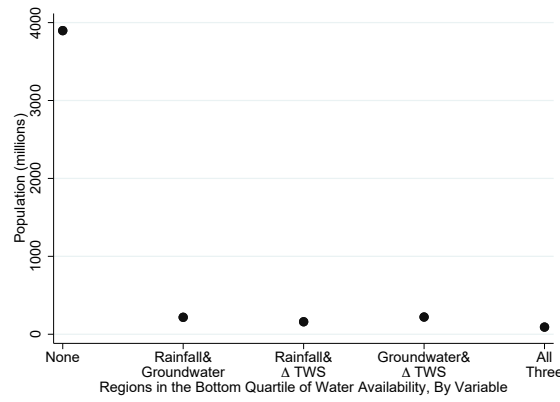


FIGURE A3. POPULATION EXPOSURE TO MULTIPLE SOURCES OF WATER STRESS

Note: Figure shows the total population over arable lands within grid cells that fall into zero, one, two, or three of the following water stress categories: (i) lowest quartile of total water storage trends; (ii) lowest quartile of average annual rainfall; (iii) lowest quartile of depth to groundwater.

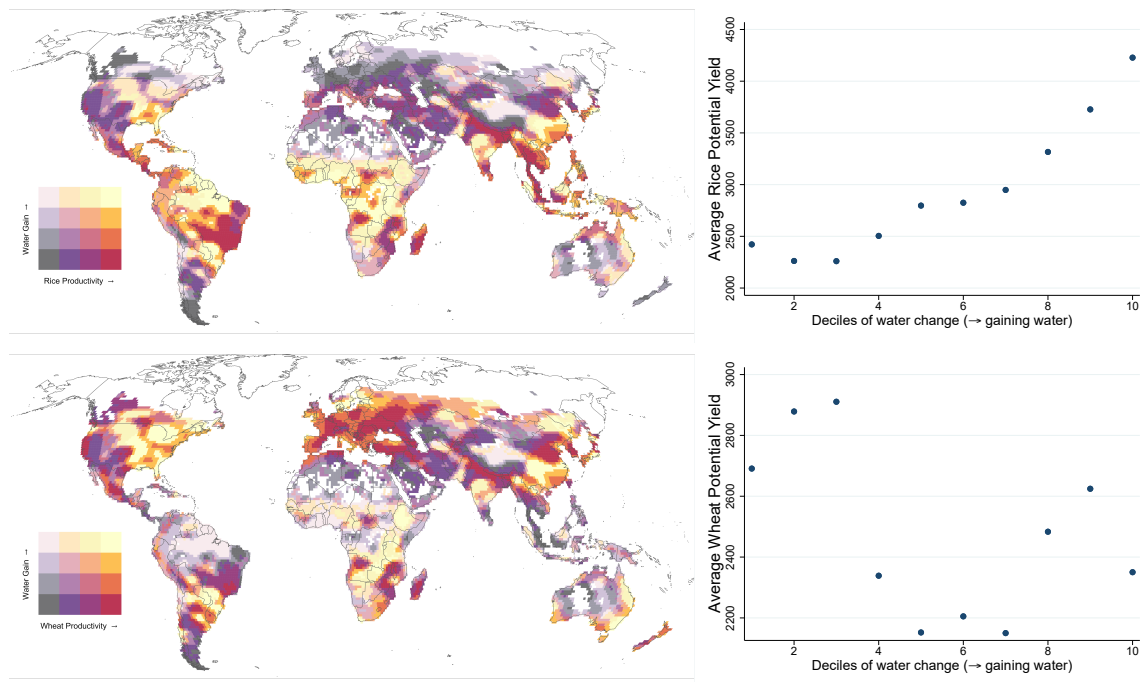


FIGURE A4. TOTAL WATER STORAGE TRENDS AND AGRICULTURAL PRODUCTIVITY: RICE AND WHEAT

Note: Top panel: Map shows trends in total water storage (centimeters of equivalent water height per year) against potential productivity of rice from GAEZ (tons/acre). Plot shows average rice potential yield in each decile of trends in total water storage across global arable lands. Bottom panel: Map shows trends in total water storage against potential productivity of wheat from GAEZ (tons/acre). Plot shows average wheat potential yield in each decile of trends in total water storage across global arable lands.

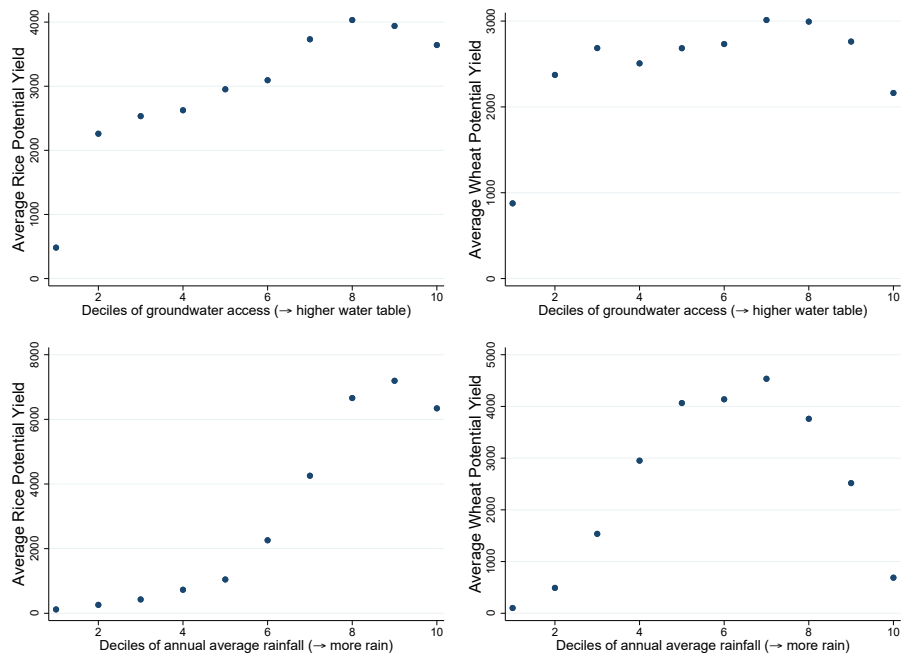


FIGURE A5. WATER STRESS AND AGRICULTURAL PRODUCTIVITY: RICE AND WHEAT

Note: Scatter plots show the average potential yield for rice (left column) and wheat (right column) in each decile of the global distribution of depth to groundwater (top row) and average annual rainfall (bottom row) over arable lands.

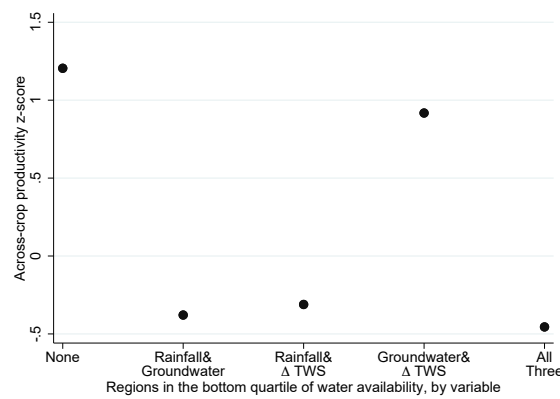


FIGURE A6. AGRICULTURAL PRODUCTIVITY IN REGIONS FACING MULTIPLE SOURCES OF WATER STRESS

Note: Figure shows the average across-crop potential agricultural productivity over arable lands within grid cells that fall into zero, one, two, or three of the following water stress categories: (i) lowest quartile of total water storage trends; (ii) lowest quartile of average annual rainfall; (iii) lowest quartile of depth to groundwater. Productivity z-scores are estimated by averaging 38 crop-specific agronomic yield estimates from GAEZ using cropped area weights from [Monfreda, Ramankutty and Foley \(2008\)](#) (see main text for details).

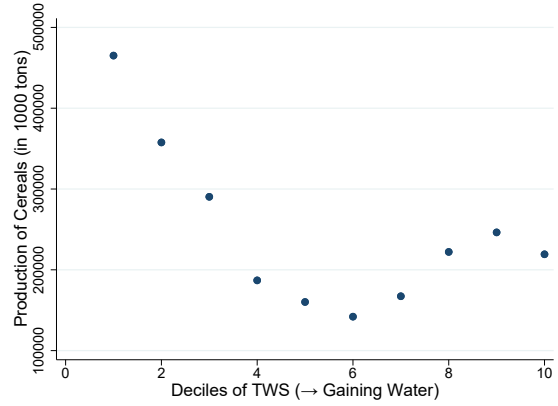


FIGURE A7. TOTAL WATER STORAGE TRENDS AND REALIZED CEREAL PRODUCTION

Note: Plot shows total quantity of cereal production in each decile of the global distribution of trends in total water storage. Cereal production is calculated using gridded estimates of realized production of wheat, rice, maize, sorghum, millet, barley, and “other cereals” from GAEZ.

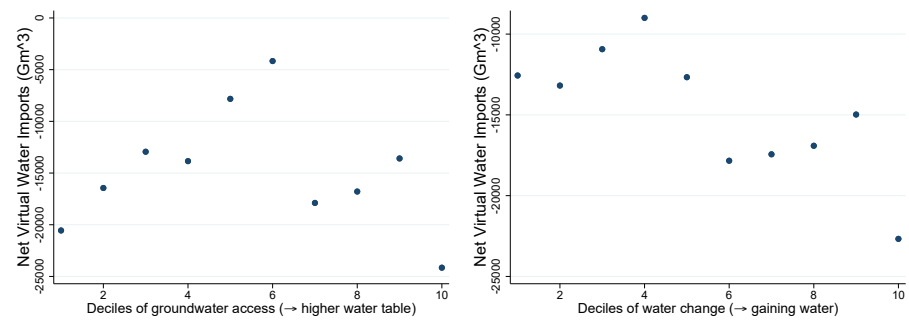


FIGURE A8. VIRTUAL WATER IMPORTS, GROUNDWATER TABLE DEPTH, AND TRENDS IN TOTAL WATER STORAGE

Note: Scatter plots show average net virtual water imports in each decile of the global distribution of depth to groundwater (left) and trends in total water storage (right). Both hydrological measures have been aggregated over the arable lands within each country before deciles are computed.

*

REFERENCES

- d'Odorico, Paolo, Joel Carr, Carole Dalin, Jampel Dell'Angelo, Megan Konar, Francesco Laio, Luca Ridolfi, Lorenzo Rosa, Samir Suweis, Stefania Tamea, and Marta Tuninetti.** 2019. "Global virtual water trade and the hydrological cycle: Patterns, drivers, and socio-environmental impacts." *Environmental Research Letters*, 14(5).
- Jacob, Thomas, John Wahr, W Tad Pfeffer, and Sean Swenson.** 2012. "Recent contributions of glaciers and ice caps to sea level rise." *Nature*, 482(7386): 514–518.
- Long, Di, Bridget R. Scanlon, Laurent Longuevergne, Alexander Y. Sun, D. Nelun Fernando, and Himanshu Save.** 2013. "GRACE satellite monitoring of large depletion in water storage in response to the 2011 drought in Texas." *Geophysical Research Letters*, 40(13): 3395–3401.
- Loomis, BD, SB Luthcke, and TJ Sabaka.** 2019. "Regularization and error characterization of GRACE mascons." *Journal of geodesy*, 93: 1381–1398.
- Mekonnen, M. M., and A. Y. Hoekstra.** 2011. "The green, blue and grey water footprint of crops and derived crop products." *Hydrology and Earth System Sciences*, 15(5): 1577–1600.
- Melton, Forrest S, Justin Huntington, Robyn Grimm, Jamie Herring, Maurice Hall, Dana Rollison, Tyler Erickson, Richard Allen, Martha Anderson, Joshua B Fisher, et al.** 2022. "OpenET: Filling a critical data gap in water management for the western United States." *JAWRA Journal of the American Water Resources Association*, 58(6): 971–994.
- Monfreda, Chad, Navin Ramankutty, and Jonathan A. Foley.** 2008. "Farming the planet: Geographic distribution of crop areas, yields, physiological types, and net primary production in the year 2000." *Global Biogeochemical Cycles*, 22(1).
- Neely, Wesley R, Adrian A Borsa, Jennifer A Burney, Morgan C Levy, Francesca Silverii, and Michelle Sneed.** 2021. "Characterization of groundwater recharge and flow in California's San Joaquin Valley from InSAR-observed surface deformation." *Water resources research*, 57(4): e2020WR028451.
- Pekel, Jean-François, Andrew Cottam, Noel Gorelick, and Alan S. Belward.** 2016. "High-resolution mapping of global surface water and its long-term changes." *Nature*, 540: 418–422.
- Proctor, Jonathan, Tamara Carleton, and Sandy Sum.** 2023. "Parameter recovery using remotely sensed variables." National Bureau of Economic Research.
- Richey, Alexandra S., Brian F. Thomas, Min-Hui Lo, John T. Reager, James S. Famiglietti, Katalyn Voss, Sean Swenson, and Matthew Rodell.** 2015. "Quantifying renewable groundwater stress with GRACE." *Water Resources Research*, 51(7): 5217–5238.
- Rodell, Matthew, Isabella Velicogna, and James S. Famiglietti.** 2009. "Satellite-based estimates of groundwater depletion in India." *Nature*, 460(7258): 999–1002.
- Rodell, M., J. S. Famiglietti, D. N. Wiese, J. T. Reager, H. K. Beaudoin, F. W. Landerer, and M.-H. Lo.** 2018. "Emerging trends in global freshwater availability." *Nature*, 557(7707): 651–659.
- Tapley, Byron D., Srinivas Bettadpur, John C. Ries, Paul F. Thompson, and Michael M. Watkins.** 2004. "GRACE measurements of mass variability in the earth system." *Science*, 305(5683): 503–505.
- Wahr, John M, Steven R Jayne, and Frank O Bryan.** 2002. "A method of inferring changes in deep ocean currents from satellite measurements of time-variable gravity." *Journal of Geophysical Research: Oceans*, 107(C12).